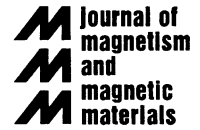




ELSEVIER

Journal of Magnetism and Magnetic Materials 223 (2001) 192–198



www.elsevier.com/locate/jmmm

Size effects on characteristic magnetic fields of a spin-valve multilayer by computer simulation

S.H. Lim*, S.H. Han, K.H. Shin, H.J. Kim

Thin Film Technology Research Center, Korea Institute of Science and Technology, P.O. Box 131, Cheongryang, Seoul 130-650, South Korea

Received 3 May 2000; received in revised form 9 October 2000

Abstract

The change in characteristic magnetic fields of a spin-valve multilayer is investigated as a function of the size by computer simulation. The spin-valve modeled in this work is IrMn (9 nm)/CoFe (4 nm)/Cu (2.6 nm)/CoFe (2 nm)/NiFe (6 nm). The spin-valve dimensions are varied widely from $20\text{ nm} \times 10\text{ nm}$ to $0.5\text{ }\mu\text{m} \times 0.25\text{ }\mu\text{m}$, but the aspect ratio defined by the ratio of the length to the width is fixed at 2.0. The magnetostatic interactions begin to affect the magnetic properties substantially at a spin-valve length of $5\text{ }\mu\text{m}$, and, at a length of $1\text{ }\mu\text{m}$, they become even more dominant. The main consequences of the magnetostatic interactions are a significant increase of the coercivity and a very large shift of the bias field in both the pinned and free layers. It is shown that these changes can be explained by two separate contributions to the total magnetostatic interactions: the coercivity change by the self-demagnetizing field and the change of the bias field by the interlayer magnetostatic interaction field. © 2001 Elsevier Science B.V. All rights reserved.

PACS: 75.50.Pa; 75.50.Ss; 75.50. – i; 85.70.K

Keywords: Spin-valve multilayer; Giant magnetoresistance; Size effects; Computer simulation; Magnetostatic interactions

1. Introduction

Spin-valve multilayers possessing giant magnetoresistance (GMR) are widely used in magnetic recording and are also considered for magnetic random access memory (MRAM) devices [1]. In magnetic recording applications, for example, the size of a spin-valve is quite small, being in the range of microns, and, with the current technology trend in the area, the size is expected to be even smaller,

possibly in the nanometer range. A similar size range is expected in an MRAM device. In this size range, it is well recognized that the magnetostatic interactions play a large role in determining the magnetic properties of the multilayers. This is clearly demonstrated by the difficulty of obtaining a suitable magnetic configuration (the crossed spin-valve configuration, for example) in patterned spin-valve read heads [2–4]. This emphasizes the importance of clearly understanding the magnetostatic interactions in a small-sized device. In the past, there were several research efforts towards this direction. Russek et al. [5] examined magnetoresistance response of spin-valves for MRAM applications in a multilayer single-domain model.

*Corresponding author. Tel.: + 82-2-958-5415; fax + 82-2-958-6851.

E-mail address: sangho@kist.re.kr (S.H. Lim).

The same model was used by Oti et al. [3] to investigate spin-valves for magnetic recording applications. A particular emphasis was placed on the deviation of the pinned-layer spin direction from the exchange bias field (or pinning field) and the resultant output of GMR signals. Micromagnetic computer simulation utilizing the Landau–Lifshitz equation was also used to investigate the role of the magnetostatic interactions in patterned spin-valves by Zheng and Zhu [6], Oti and Russek [7], and Mao et al. [8]. It was shown from these previous researches that a significant change in the magnetic and magnetoresistance properties occurs with the spin-valve size, demonstrating the importance of the magnetostatic interactions in the small-size range. The previous work, however, was mainly focused on the variation of the magnetostatic interactions with the aspect ratio (defined as the ratio of the length to the width). In most cases, the width was fixed at a certain value, but the length was changed to vary the aspect ratio. The size itself and the aspect ratio, which are two main factors affecting the magnetostatic interactions, were varied simultaneously in the previous work, making it difficult to analyze the results. Also, the range of the spin-valve size investigated was very much limited, making it hard to understand the overall picture of the size dependence of the magnetostatic interactions and hence magnetic properties of spin-valve multilayers. In an effort to rectify this situation, a systematic investigation is carried out in this work, through computer simulation, by varying the size of a spin-valve multilayer over a wide range while maintaining the aspect ratio constant.

2. Model and computation

In the model, each magnetic layer consists of a single domain, indicating that the magnetization is uniform within a layer. The spin-valve modeled in this work is IrMn (9 nm)/CoFe (4 nm)/Cu (2.6 nm)/CoFe (2 nm)/NiFe (6 nm). In order to see the size effects, the multilayer dimensions are varied widely from $20\text{ nm} \times 10\text{ nm}$ to $0.5\text{ }\mu\text{m} \times 0.25\text{ }\mu\text{m}$. It is noted that the aspect ratio is fixed at 2.0 in all cases. The unidirectional pinning field (H_{pin}) acting on the pinned layer is 280 Oe. The magnitude of the

uniaxial-induced anisotropy is 46 Oe in the pinned layer ($H_{\text{A,p}}$) and is 5 Oe in the two free layers ($H_{\text{A,f}}$). The direction of H_{pin} , $H_{\text{A,p}}$ and $H_{\text{A,f}}$ is parallel to the length direction. Magnetic layers are coupled through the magnetostatic and interlayer exchange interactions. The ferromagnetic exchange coupling (H_{exch}) (more specifically, the Néel orange peel coupling the origin of which is magnetostatic interactions in nature) exists between the pinned and free layers and its magnitude is 12 Oe. The magnetization of the CoFe layers is taken as 1300 emu/cm^3 and that of NiFe as 800 emu/cm^3 . In the actual calculation, the two free layers (CoFe (2 nm) and NiFe (6 nm)) are treated as a single layer, for calculational simplicity, with an average magnetization of 925 emu/cm^3 . This indicates that one of the free layers exactly follows the other, which is in agreement with experimental observations for this type of spin-valves. This assumption is expected to affect detailed magnetostatic interactions, but will not influence the main conclusion of this work. Neither the magnetic field from sensing currents nor the hard-biased field (which is used to stabilize the domain of the free layer) is considered in this model. The change in magnetoresistance is calculated by using the expression $\Delta R = 1 - \cos \theta$, where θ is the angle between the magnetization directions of the pinned and free layers. The magnetic field is applied in the length direction and is cycled between + 500 and – 500 Oe (a higher field is also applied in some cases). The present multilayers are relevant to an MRAM cell, rather than a spin-valve read head used in magnetic recording, the applied field (H_a) being parallel to the pinning field and the anisotropy field.

3. Results and discussion

The change in the magnetic properties was investigated mainly by measuring M – H hysteresis loops, and some of the results are shown in Figs. 1(a)–(d) for several spin-valves, $20\text{ nm} \times 10\text{ nm}$, $20\text{ }\mu\text{m} \times 10\text{ }\mu\text{m}$, $5\text{ }\mu\text{m} \times 2.5\text{ }\mu\text{m}$ and $1\text{ }\mu\text{m} \times 0.5\text{ }\mu\text{m}$, respectively. The M – H loops obtained from the smallest spin-valve of $1\text{ }\mu\text{m} \times 0.5\text{ }\mu\text{m}$ are also shown in Fig. 1(a) together with the largest spin-valve of $20\text{ nm} \times 10\text{ nm}$, in order to emphasize the

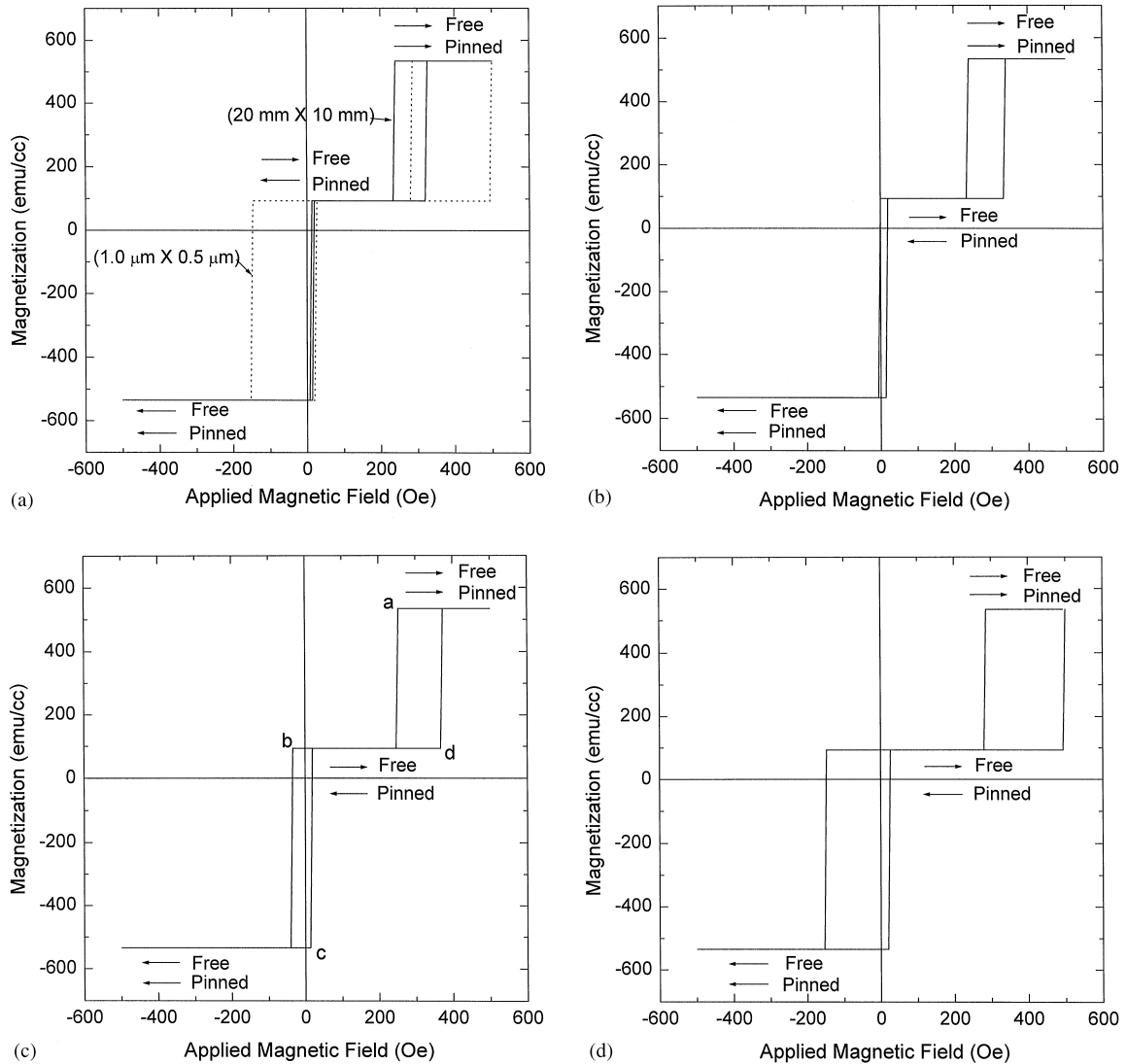


Fig. 1. M - H hysteresis loops for several spin-valve dimensions: (a) $20\text{ mm} \times 10\text{ mm}$; (b) $20\text{ }\mu\text{m} \times 10\text{ }\mu\text{m}$; (c) $5\text{ }\mu\text{m} \times 2.5\text{ }\mu\text{m}$; and (d) $1\text{ }\mu\text{m} \times 0.5\text{ }\mu\text{m}$. The M - H loops obtained for the smallest spin-valve of $1\text{ }\mu\text{m} \times 0.5\text{ }\mu\text{m}$ are also shown in (a) for comparison.

difference of the loops. It is seen from the figures that, indeed, a significant difference is observed to exist in the M - H loops. A prominent phenomenon common to all is that the magnetization changes abruptly by spin-flip. This is expected, since the direction of H_a is parallel to all the unidirectional and uniaxial anisotropy fields.

Several characteristic fields can be identified from the loops; the coercivities of the pinned and

free layers ($H_{c,p}$ and $H_{c,f}$, respectively) and the bias fields of the pinned and free layers ($H_{\text{bias,p}}$ and $H_{\text{bias,f}}$, respectively). In the case of the largest spin-valve of $20\text{ mm} \times 10\text{ mm}$, the values of the characteristic fields are identical to those expected from the values of $H_{A,p}$, $H_{A,f}$, H_{pin} and H_{exch} . Specifically, the values of the coercivity are equal to the uniaxial anisotropy fields in the respective layers ($H_{c,p} = H_{A,p} = 46\text{ Oe}$; $H_{c,f} = H_{A,f} = 5\text{ Oe}$),

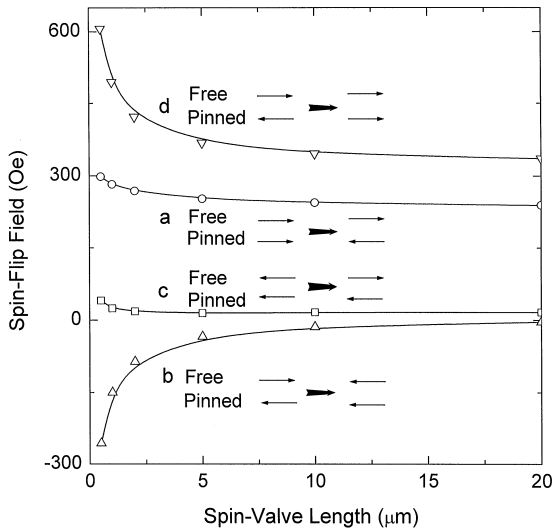


Fig. 2. The applied magnetic fields at which spin-flip occurs as a function of the spin-valve length. The spin-flip positions of *a–d* are indicated in the *M–H* loops of Fig. 1(c).

and the bias fields are identical to the unidirectional exchange fields ($H_{\text{bias,p}} = H_{\text{pin}} = 280$ Oe; $H_{\text{bias,f}} = H_{\text{exch}} = 12$ Oe). However, as the multilayer size decreases, these characteristic fields change significantly. In order to see the size dependence of these characteristic fields more clearly, the magnetic fields at which spin-flip occurs in the *M–H* loops are plotted as a function of the size, and these results are shown in Fig. 2. The spin-flip positions of *a–d* in Fig. 2 are indicated in the *M–H* loops in Fig. 1(c). In Fig. 2, the spin-valve size (the *x*-axis) is indicated only by the length (the long dimension of the device). The following relationships exist between the spin-flip fields and the characteristic fields; $H_{\text{c,p}} = (d - a)/2$, $H_{\text{c,f}} = (c - b)/2$, $H_{\text{bias,p}} = (a + d)/2$, and $H_{\text{bias,f}} = (b + c)/2$.

From Figs. 1 and 2, it is seen that the spin-flip positions of *a* and *c* vary slightly with the size, but, the other positions of *b* and *d* vary significantly with the dimension. The small size dependence of the spin-flip fields of *a* and *c*, compared with that of *b* and *d*, is considered to be related with the spin configuration. The spin-flip positions of *a* and *c* correspond to magnetization change from parallel spin configuration to antiparallel one. The situation is opposite at the spin-flip positions of

b and *d*. Spin-flip from antiparallel-to-parallel spin configuration is considered to be more difficult than the opposite direction, since the interlayer magnetostatic interaction field (H_{ms}) favors the antiparallel spin configuration. At the spin-flip position *b*, for example, the free layer spin rotates towards the $-x$ direction, the same direction of the pinned spin. The spin rotation will occur at $H_a = +7$ Oe, provided no magnetostatic interactions exist. This rotation of the free layer, however, will occur at a large H_a value, since H_{ms} from the pinned layer acts on the free layer in the $+x$ direction, making it difficult for the free layer spin to rotate.

Over the whole size range investigated in this work, the variation of the spin-flip field with size is as follows: $a = 234\text{--}298$ Oe; $b = 7\text{--}256$ Oe; $c = 16\text{--}40$ Oe; $d = 325\text{--}606$ Oe. It is interesting to see that the change of the characteristic fields related to the free layer (*b* and *c*) is slightly smaller than that related to the pinned layer (*a* and *d*). In the case of the spin-flip positions of *b* and *d*, where a large size dependence is observed, the change of the spin-flip fields is actually not very significant as the spin-valve length changes from 20 mm to 5 μm . Below this dimension, however, a significant change is observed, the variation being even greater as the length becomes smaller than 1 μm . This size dependence of *M–H* hysteresis loops (or in other words, the spin-flip fields) is obviously related to the magnetostatic interaction fields which can be divided into the self-demagnetizing field (H_{demag}) and H_{ms} already mentioned in the previous paragraph.

The increase of the coercivity with the decrease of the spin-valve size, which can be easily obtained from the results shown in Fig. 2 for the size dependence of the spin-flip fields, can be explained by the change of the uniaxial shape anisotropy. Although, in this work, the aspect ratio (the length/width ratio) is fixed at 2 for all the samples, the value of H_{demag} in the length direction is different from that in the width direction, and, furthermore, the difference in the values of H_{demag} in the two directions increases with decreasing size. The difference in the values of H_{demag} in the two principal directions corresponds to the shape anisotropy, which is uniaxial in nature. In Figs. 3(a) and (b) are shown

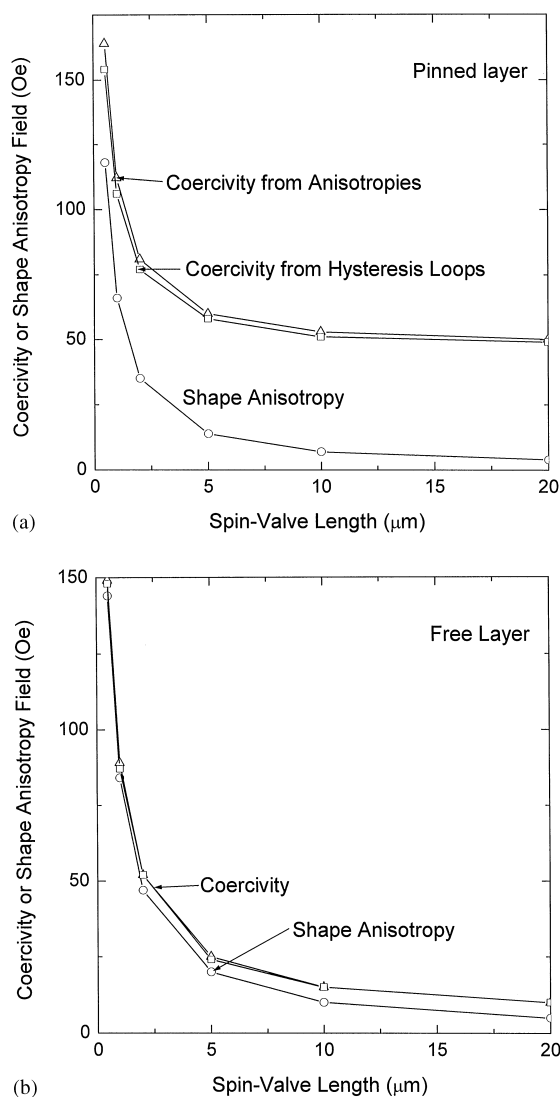


Fig. 3. The shape anisotropy (circles), and the two sets of the coercivities, one obtained from the hysteresis loops (squares) and the other from the shape anisotropy (triangles), as a function of the spin-valve length for (a) the pinned layer, and (b) the free layer.

the results for the shape anisotropy in the pinned and free layers, respectively. The magnitude of the coercivity in each layer is then expected to be the sum of the (uniaxial) induced anisotropy and the shape anisotropy. The coercivity obtained in this way is also shown in the figures, together with those obtained from the hysteresis loops.

From Figs. 3(a) and (b) it is seen that a very large size dependence on the shape anisotropy and the coercivity is observed, in a way similar to the results shown in Fig. 2 for the spin-flip field. The magnitude of the shape anisotropy is nearly zero at the largest spin-valve of $20\text{ mm} \times 10\text{ mm}$, but it increases exponentially with the decrease of the size. The magnitude of the shape anisotropy is greater in the free layer than that in the pinned layer, in spite of a smaller saturation magnetization of the free layer. This is because the free layer is thicker than the pinned layer and hence the difference of the demagnetization coefficients in the length and the width direction is greater in the case of the free layer. In the case of the free layer, the value of $H_{c,f}$ obtained from the results shown in Figs. 1 and 2 for the hysteresis loop is in excellent agreement with that from the shape anisotropy (the sum of the shape anisotropy and 5 Oe for the induced anisotropy). In the case of the pinned layer, however, the magnitude of $H_{c,p}$ from the hysteresis loop is lower than that estimated from the shape anisotropy (the sum of the anisotropy and 46 Oe for the induced anisotropy). The discrepancy between the two increases with decreasing size. The reason for this discrepancy is not clearly understood at this moment. Considering that the coercivity is equal to the total (uniaxial) anisotropy only for the condition that magnetization change occurs by a complete spin-flip, the spin-flip behavior in the pinned layer may deviate from this ideal flip and the ideality increases with decreasing size. In this sense, the value of the coercivity obtained from the sum of all the uniaxial anisotropies is considered to be the upper limit of this magnetic parameter.

Let us now consider the bias (or offset) fields of the pinned and free layers. In the absence of the magnetostatic interactions such as the case for the $20\text{ mm} \times 10\text{ mm}$ spin-valve, the bias fields of the pinned and free layers are, respectively, +280 and +12 Oe. However, these bias fields change in the presence of magnetostatic interactions. It is observed that, over the whole size range, the change of the bias field is completely explained by the change of H_{ms} , the results for which are shown in Figs. 4(a) and (b) in the pinned and free layers, respectively. Also shown in the figures are the values of H_{bias} obtained from the hysteresis loops and H_{ms} .

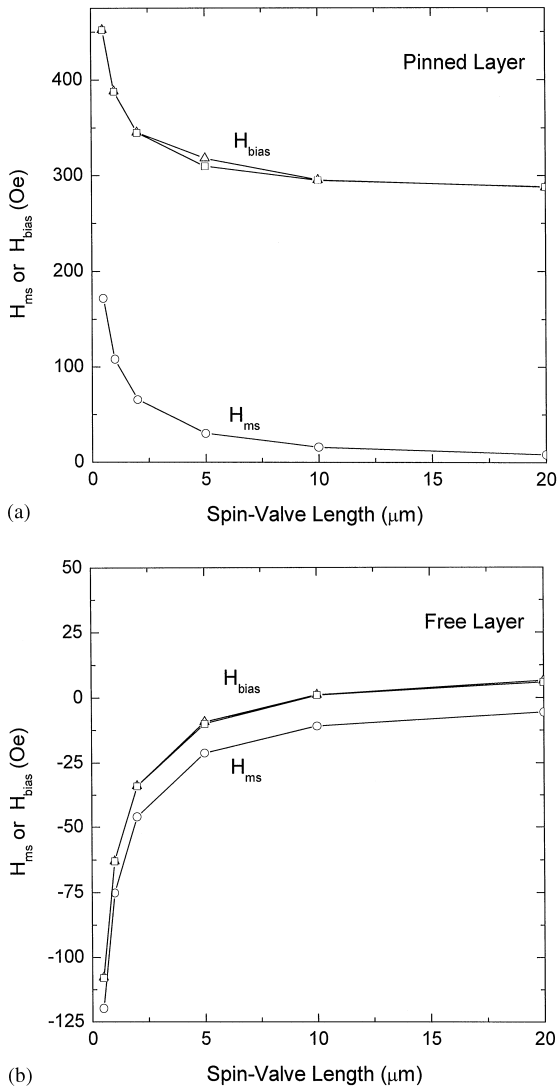


Fig. 4. The interlayer magnetostatic interaction field (circles), and the two sets of the bias fields, one obtained from the hysteresis loops (squares) and the other from the interlayer magnetostatic interaction field (triangles), as a function of the spin-valve length for (a) the pinned layer, and (b) the free layer.

Again, the size dependence of H_{ms} is similar to those observed for spin-flip field and the shape anisotropy. The value of $H_{bias,p}$ can be obtained by adding H_{pin} (280 Oe) to H_{ms} acting on the pinned layer, resulting in a very large positive $H_{bias,p}$ value; for example, + 452 Oe in the smallest spin-valve of $0.5 \mu\text{m} \times 0.25 \mu\text{m}$. The bias field obtained in this

way is in perfect agreement with that obtained from the results shown in Figs. 1 and 2 for the hysteresis loop. In the case of the free layer, the bias field can be obtained by adding H_{ms} to H_{exch} (12 Oe). Since the value of H_{ms} at small sizes is a large negative value, $H_{bias,f}$ in this case is a large negative value; - 108 Oe in the smallest spin-valve of $0.5 \mu\text{m} \times 0.25 \mu\text{m}$. Again, the magnitude of H_{bias} obtained from H_{ms} is in excellent agreement with that obtained from the hysteresis loops. This relationship between H_{bias} and H_{ms} can be understood, since H_{ms} is unidirectional in nature, like the pinning field and the exchange field. It is worth noting that the value of H_{ms} acting on the pinned layer is greater than that acting on the free layer. This can be understood, since the product of the thickness and saturation magnetization of the free layer, to which the value of H_{ms} acting on the pinned layer is proportional, is greater than that of the pinned layer.

The magnetoresistance properties of the present spin-valves can easily be estimated from the $M-H$ loops since the magnetization occurs only by spin-flip. In the case of the spin-valve shown in Fig. 1(c), for example, as H_a decreases from 500 Oe to a , the spins in the pinned and free layers are parallel to each other and hence the magnetoresistance is minimum. The magnetoresistance becomes maximum in the H_a range from a to b where the spins are antiparallel. At H_a values lower than b , the magnetoresistance is minimum again.

As was already pointed out in the previous section, the magnetic configuration of the present spin-valve is relevant to an MRAM cell. Since the size of an MRAM cell is expected to be in the submicron range [9], it is expected from the present results that the magnetic properties of a spin-valve in an MRAM device are affected significantly by the magnetostatic interactions, one typical example being a very large coercivity. However, it is important to note at this stage that, in a real MRAM device, the change of the characteristic fields will not be that great, compared with that observed in this model. This is because a real spin-valve even with a submicron size may have a complicated spin structure, not a simple single domain structure, in a way to reduce the magnetostatic interactions. One example of the complicated spin structure is

the magnetization curling formed at the edge of the layers [6,7]. With the presence of the complicated spin structure, the magnetization change will not occur abruptly by spin-flip, causing the coercivity to decrease, among many others. In this sense, the present results for the characteristic fields are considered to provide the upper limit; in other words, the values of the coercivity and bias field obtained at a given spin-valve size are always greater than those observed in real devices. It is rather ironic to see that this complicated spin-structure obtained in a more realistic model provides an obstacle to the clear understanding of an overall picture on the size dependence of the magnetic properties. Due to small magnetostatic interactions at large sizes, the difference in the values between the model calculations and experiments is expected to be small in this size range. As the size of a magnetic material becomes very small, a single-domain state is favored. In this size range, this difference will also be small, indicating that the present single-domain model works well.

4. Conclusions

Computer simulation has been carried out in this work to examine the size dependence of the magnetic properties of a spin-valve multilayer. The size of the spin-valve is varied widely from $20\text{ nm} \times 10\text{ nm}$ to $0.5\text{ }\mu\text{m} \times 0.25\text{ }\mu\text{m}$ while maintaining the aspect ratio (the ratio of the length to the width) fixed at 2.0. The spin-valve modeled in this work is IrMn (9 nm)/CoFe (4 nm)/Cu (2.6 nm)/CoFe (2 nm)/NiFe (6 nm). M - H hysteresis loops of spin-valves of various sizes indicate that, at small lengths below $5\text{ }\mu\text{m}$, characteristic magnetic fields such as the coercivity and the bias field vary significantly with the spin-valve size in both the pinned and free layers, and the variation is even greater at lengths below $1\text{ }\mu\text{m}$. This size dependence of the magnetic properties is due to the magnetostatic interactions which arise from the discontinuity of the magnetization. Two separate field compo-

nents, the self-demagnetizing field and the interlayer magnetostatic interaction field, can be identified from the magnetostatic interactions, and it has been shown that the change of the coercivity and the bias field can be explained, respectively, by the self-demagnetizing field and the interlayer magnetostatic interaction field. The coercivities in both the pinned and free layers obtained from the hysteresis loops are in good agreement with those estimated from the uniaxial shape anisotropy which is defined as the difference of the self-demagnetizing fields in the width and the length directions. Also, the bias fields in the two magnetic layers are in excellent agreement with those estimated from the unidirectional interlayer magnetostatic interaction field.

Acknowledgements

The simulation was performed with a program developed at NIST by Dr. John Oti (now at Euxine Technologies). Financial support from the National Research Laboratory Program (Magnetic Thin Film Laboratory) and the Nano Functional Devices Program (a 21C Frontier R&D Project) is gratefully acknowledged.

References

- [1] D.D. Tang, P.K. Wang, V.S. Speriosu, S. Le, K.K. Kung, IEEE Trans. Magn. 31 (1995) 3206.
- [2] R.W. Cross, Y. Kim, J.O. Oti, S.E. Russek, Appl. Phys. Lett. 69 (1996) 3935.
- [3] J.O. Oti, R.W. Cross, S.E. Russek, Y.K. Kim, J. Appl. Phys. 79 (1996) 6386.
- [4] S.H. Lim, K.H. Shin, K.Y. Kim, S.H. Han, H.J. Kim, J. Magn. 5 (2000) 19.
- [5] S.E. Russek, J.O. Oti, Y.K. Kim, R.W. Cross, IEEE Trans. Magn. 33 (1997) 3292.
- [6] Y. Zheng, J.G. Zhu, IEEE Trans. Magn. 32 (1996) 4237.
- [7] J.O. Oti, S.E. Russek, IEEE Trans. Magn. 33 (1997) 3298.
- [8] S. Mao, J. Giusti, N. Amin, J. Van ek, Ed. Murdock, J. Appl. Phys. 85 (1999) 6112.
- [9] T.N. Fang, J.G. Zhu, IEEE Trans. Magn. 35 (1999) 2835.